

Synthesis, characterization, DNA interaction and in vitro cytotoxicity activities of ruthenium(II) Schiff base complexes

Subbaiyan Sathiyaraj^a, Ray J. Butcher^b, Chinnasamy Jayabalakrishnan^{a,*}

^a Post Graduate and Research Department of Chemistry, Sri Ramakrishna Mission Vidyalaya College of Arts and Science, Coimbatore 641 020, Tamil Nadu, India

^b Department of Chemistry, Howard University, Washington, DC 20059, USA

HIGHLIGHTS

- ▶ Preparation of Schiff base ligand and its ruthenium(II) complexes.
- ▶ Structure of ligand was confirmed by X-ray analysis.
- ▶ DNA interaction and in vitro cytotoxicity activities were carried out.
- ▶ Ruthenium(II) complexes show more binding ability than the ligand.
- ▶ Ligand and the complexes showed better cytotoxicity against HeLa cancer cell line.

ARTICLE INFO

Article history:

Received 16 February 2012

Received in revised form 30 April 2012

Accepted 13 July 2012

Available online 26 July 2012

Keywords:

Ruthenium(II) complexes

Aminobenzothiazole

Crystal structure

DNA-interaction

Cytotoxicity

ABSTRACT

DNA binding, cleavage and cytotoxicity characteristics of a novel Schiff base ligand 3-(benzothiazol-2-yliminomethyl)-naphthalen-2-ol and ruthenium(II) complexes have been investigated. The DNA interaction properties of the complexes have been investigated using absorption spectra, as well as gel electrophoresis studies. Intrinsic binding constant (K_b) has been estimated under similar set of experimental conditions. Absorption spectral study indicate that the ligand and ruthenium(II) complexes has intrinsic binding constant in the range of $1.4\text{--}7.2 \times 10^4 \text{ M}^{-1}$. Ruthenium(II) complexes show more binding ability than the ligand. Further, in vitro cytotoxicity study of the ligand and the complexes exhibited antitumor activity against HeLa and HEP2 tumor cells.

© 2012 Elsevier B.V. All rights reserved.

1. Introduction

In recent years, many researches [1–3] have been focused on interaction of small molecules with DNA. DNA is generally the primary intracellular target of anticancer drugs, so the interaction between small molecules and DNA can cause DNA damage in cancer cells, blocking the division of cancer cells, and resulting in cell death [4,5]. Small molecule can interact with DNA through the following three non-covalent modes: intercalation, groove binding and external static electronic effects. Among these interactions, intercalation is one of the most important DNA-binding modes, which is related to the antitumor activity of the compound. Recently, there is a great interest on the binding of transition metal complexes with DNA, owing to their possible applications as new cancer therapeutic agents and their photochemical properties that make them potential probes of DNA structure and conformation

[6–8]. It has been reported that the intercalating ability of the complex was involved in the planarity of ligands, the coordination geometry, ligand donor atom type, the metal ion type [9–11]. So the development of synthetic, sequence-selective DNA binding and cleavage agents for DNA itself and for new potential DNA-targeted antitumor drugs is essential for further expected applications in molecular biology, medicine, and related fields. Schiff bases form an interesting class of ligands that has enjoyed popular use in the coordination chemistry of transition, inner transition and main group elements [12,13]. Schiff bases have been reported to show a variety of biological actions by virtue of the azomethine linkage, which is responsible for various antibacterial, antifungal, herbicidal and clinical activities [14–16]. Benzothiazole ring is present in various marine or terrestrial natural compounds which have useful biological activities [17]. Transition metal ions play a vital role in a vast number of widely different biological processes. In particular, ruthenium complexes are better suited for medical applications because of their favorable rate of ligand exchange and their ability to mimic iron binding to certain biomolecules

* Corresponding author. Tel.: +91 422 2692461.

E-mail address: cjayabalakrishnan@gmail.com (C. Jayabalakrishnan).

[18]. Metal complexes of Schiff bases derived from heterocyclic compounds containing nitrogen, sulfur and/or oxygen as ligand atoms are of interest as simple structural models of more complicated biological systems [19].

Herein, we report the synthesis, characterization, DNA binding, cleavage and cytotoxic abilities of ruthenium(II) complexes containing 3-(benzothiazol-2-yliminomethyl)-naphthalen-2-ol. Schiff base derived from 2-aminobenzothiazole and 2-hydroxy-1-naphthaldehyde. Schiff base was structurally characterized by single crystal X-ray crystallography.

2. Experimental

2.1. Materials and instrumentation

Reagent grade chemicals were used without further purification in all the synthetic work. All solvents were purified by standard methods. 2-hydroxy-1-naphthaldehyde, 2-amino benzothiazole were purchased from Sigma–Aldrich chemie. $\text{RuCl}_3 \cdot 3\text{H}_2\text{O}$, triphenyl phosphine/arsine were purchased from Himedia. Calf-thymus (CT-DNA) was purchased from Bangalore Genei, Bangalore, India. The Human Cervical cancer cell line HeLa and human laryngeal epithelial carcinoma cell line HEP2 were obtained from National center for cell science (NCCS), pune, India.

Infrared spectra were recorded on a FT-IR Perkin Elmer spectrophotometer RXI model as KBR pellets in the range $4000\text{--}400\text{ cm}^{-1}$. Elemental analyses were performed with a model Vario ELIII CHNS at Sophisticated Test and Instrumentation Centre (STIC), Cochin University, Kerala. Electronic spectra were recorded in DMSO solution in a Systronics 2202 Double beam spectrophotometer in $800\text{--}200\text{ nm}$ range. ^1H , ^{13}C and ^{31}P NMR spectra were recorded on Bruker WM DCX 500 MHz instrument using TMS and ortho phosphoric acid as an internal standard at SAIF, Indian Institute of Technology, Chennai. Anti cancer studies was carried out at the Kovai Medical Centre and Hospital Pharmacy College, Coimbatore, Tamil Nadu.

2.2. Crystal structure determination

Single crystal of Schiff base ligand (HL) was grown by slow evaporation of a solution of the ligand in chloroform. Selected crystal data are given in Tables 1 and 2, Fig. 1. The X-ray diffraction data for ligand (HL) were collected on a Bruker SMART CCD diffraction using graphite-monochromated $\text{Mo K}\alpha$ radiation ($\lambda = 0.71073\text{ \AA}$) by φ and ω scans. X-ray data reduction structure solution and refinement were done using the SHEL XS-97 and SHELXL-97 packages [20]. The structure was solved by direct methods.

2.3. Synthesis of the Schiff base ligand

The Schiff base ligand 3-(benzothiazol-2-yliminomethyl)-naphthalen-2-ol (HL) was isolated from the condensation reaction of 2-hydroxy-1-naphthaldehyde (1.20 g, 10 mmol) and 2-amino benzothiazole (1.5 g, 10 mmol) in ethanol under reflux for 6 h. After cooling the reaction mixture to room temperature, the solid product formed was filtered, washed with ethanol and dried in *vacuo* (Scheme 1). Yield 72%; Color: Orange; M.P: $148\text{ }^\circ\text{C}$. This solid was recrystallized from chloroform, yielding orange crystals suitable for X-ray diffraction analysis. Anal. Calc for $\text{C}_{18}\text{H}_{12}\text{N}_2\text{O}_2$: C, 70.02; H, 4.61; N, 9.15; S, 10.46. Found: C, 70.30; H, 4.33; N, 8.92; S, 10.12. IR (cm^{-1}): 3396 (ph-OH), 1622 (C=N), 1599 (C=N thiazole ring), 1311 (ph-CO). UV-vis (in DMSO); λ_{max} , nm; 276, 365, 445, 476. ^1H NMR (ppm); 8.72 (1H, s, HC=N), 10.12 (1H, s, Ar-OH), 7.24–8.27 (m, Ar-H). ^{13}C NMR (ppm); 152 (C=N imine), 166 (C=N thiazole), 117–136 (Ar-C).

Table 1
Crystal and structure refinement data for Schiff base ligand (HL).

Empirical formula	$\text{C}_{18}\text{H}_{12}\text{N}_2\text{O}_2\text{S}$
Formula weight	304.36
Temperature	295(2) K
Wavelength	0.71073 \AA
Crystal system	Monoclinic
Space group	$P 2_1/n$
<i>Unit cell dimensions</i>	
<i>a</i> (\AA)	9.7176(3)
<i>b</i> (\AA)	15.0806(6)
<i>c</i> (\AA)	9.7882(3)
α ($^\circ$)	90
β ($^\circ$)	101.713(3)
γ ($^\circ$)	90
Volume	1404.56(8) \AA^3
Density (calculated)	1.439 Mg/m^3
Crystal size	$0.47 \times 0.38 \times 0.24\text{ mm}^3$
Theta range for data collection	$5.13\text{--}34.98^\circ$
Index ranges	$-15 < h < 14$ $-19 < k < 24$ $-15 < l < 14$
Reflections collected	12583
Independent reflections	5739 [$R(\text{int}) = 0.0261$]
Refinement method	Full-matrix least-squares on F^2
Data/restraints/parameters	5739/0/200
Goodness-of-fit on F^2	1.035
Final <i>R</i> indices [$I > 2\sigma(I)$]	$R1 = 0.0557$, $wR2 = 0.1303$
<i>R</i> indices (all data)	$R1 = 0.0956$, $wR2 = 0.1518$
Largest diff. peak and hole	0.353 and $-0.243\text{ e}\cdot\text{\AA}^{-3}$

Table 2
Selected Bond lengths (\AA) and angles ($^\circ$) for Schiff base ligand (HL).

Bond lengths		Bond angles	
S(1)–C(18)	1.7332(16)	C(18)–S(1)–C(12)	88.78(7)
S(1)–C(12)	1.7462(14)	C(1)–O(1)–H(1A)	109.5
O(1)–C(1)	1.3348(18)	C(11)–N(1)–C(12)	117.79(12)
O(1)–H(1A)	0.8200	C(12)–N(2)–C(13)	110.50(12)
N(1)–C(11)	1.3023(18)	O(1)–C(1)–C(10)	122.51(13)
N(1)–C(12)	1.3943(19)	O(1)–C(1)–C(2)	116.80(13)
N(2)–C(12)	1.2941(19)	C(10)–C(1)–C(2)	120.69(14)
N(2)–C(13)	1.3870(18)	C(3)–C(2)–C(1)	120.06(15)
C(1)–C(10)	1.406(2)	C(3)–C(2)–H(2A)	120.0
C(1)–C(2)	1.412(2)	C(1)–C(2)–H(2A)	120.0
C(2)–C(3)	1.353(2)	C(2)–C(3)–C(4)	122.15(14)
C(2)–H(2A)	0.9300	C(2)–C(3)–H(3A)	118.9
C(3)–C(4)	1.422(2)	C(4)–C(3)–H(3A)	118.9
C(3)–H(3A)	0.9300	C(5)–C(4)–C(9)	119.99(14)
C(4)–C(5)	1.408(2)	C(5)–C(4)–C(3)	121.16(14)
C(4)–C(9)	1.418(2)		

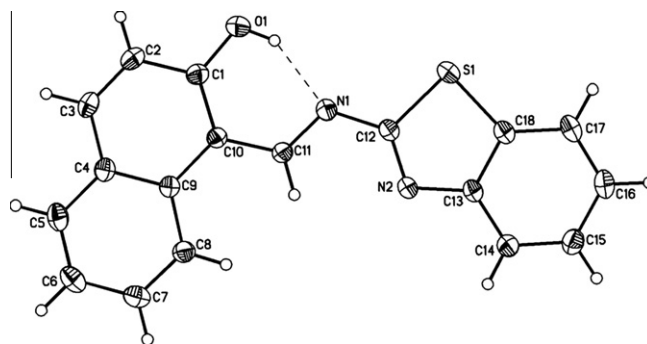
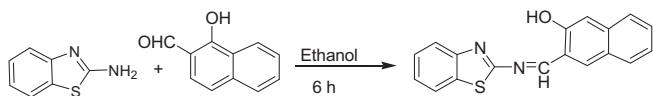


Fig. 1. ORTEP for HL.

2.4. Synthesis of $[\text{RuCl}(\text{CO})(\text{PPh}_3)_2\text{L}]$ (1)

To a solution of Schiff base ligand (HL) (0.060 g, 0.2 mmol) in methanol (20 cm^3) was added triethylamine (0.020 g, 0.2 mmol)



Scheme 1. Formation of Schiff base ligand PPh₃ (Triphenyl phosphine); AsPh₃ (Triphenyl arsine); py (pyridine).

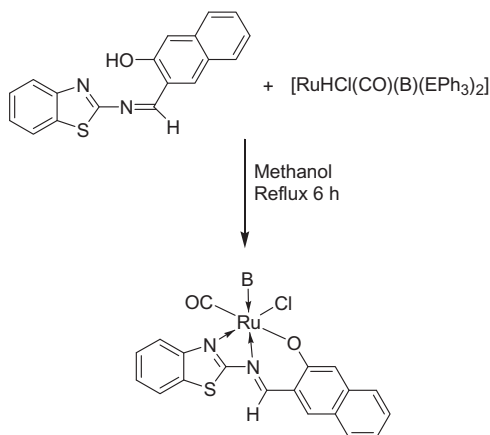
followed by [RuHCl(CO)(PPh₃)₃] [21] (1.91 g, 0.2 mmol) and the mixture was refluxed for 6 h to afford a reddish orange solution. The solvent was then evaporated under reduced pressure and the solid mass, thus obtained, was subjected to purification by TLC. This solid was recrystallized from CH₂Cl₂/Hexane mixture. Our sincere effort to obtain single crystal of the complexes went unsuccessful. Yield: 58%; Color: reddish brown; M.P: 155 °C. Anal. Calc for C₃₇H₂₆ClN₂O₂PRuS: C, 60.86; H, 3.59; N, 3.84; S, 4.39. Found: C, 60.65; H, 3.25; N, 3.52; S, 4.12. IR (cm⁻¹); 1618 (C=N), 1573 (C=N thiazole ring), 1350 (ph-CO), 1925 (C=O). UV-vis (in DMSO); λ_{max}, nm; 252, 296, 365, 416, 524. ¹H NMR (ppm); 9.12 (1H, s, HC=N), 6.26–7.83 (m, Ar-H). ¹³C NMR (ppm); 162 (C=N imine), 170 (C=N thiazole), 194 (C=O), 128–138 (Ar-C).

2.5. Synthesis of [RuCl(CO)(AsPh₃)₂L] (2)

Complex **2** was synthesized as described for (**1**) by utilizing [RuHCl(CO)(AsPh₃)₃] [22] (2.168 g; 0.2 mmol) and the Schiff base ligand (HL) (0.060 g; 0.2 mmol) as in Scheme 2. Yield: 63%; Color: orange; M.P: 190 °C. Anal. Calc for C₃₇H₂₆ClN₂O₂AsRuS: C, 57.41; H, 3.39; N, 3.62; S, 4.14. Found: C, 57.30; H, 3.15; N, 3.47; S, 4.08. IR (cm⁻¹); 1598 (C=N), 1578 (C=N thiazole ring), 1324 (ph-CO), 1965 (C=O). UV-vis (in DMSO); λ_{max}, nm; 252, 296, 361, 445, 531. ¹H NMR (ppm); 9.02 (1H, s, HC=N), 7.08–8.12 (m, Ar-H). ¹³C NMR (ppm); 159 (C=N imine), 169 (C=N thiazole), 191 (C=O), 114–134 (Ar-C).

2.6. Synthesis of [RuCl(CO)(py)L] (3)

Complex **3** was synthesized as described for (**1**) by utilizing [RuHCl(CO)py(PPh₃)₂] [23] (1.538 g; 0.2 mmol) and the Schiff base ligand (HL) (0.060 g; 0.2 mmol) as in Scheme 2. Yield: 54%; Color: brown; M.P: 182 °C. Anal. Calc for C₂₄H₁₆ClN₃O₂RuS: C, 52.70; H, 2.95; N, 7.68; S, 5.58. Found: C, 52.95; H, 2.77; N, 7.61; S, 5.68. IR (cm⁻¹); 1604 (C=N), 1575 (C=N thiazole ring), 1338 (ph-CO), 1938 (C=O). UV-vis (in DMSO); λ_{max}, nm; 255, 294, 347, 432,



where, B=PPh₃/AsPh₃/py; E=PPh₃/AsPh₃

PPh₃ (Triphenyl phosphine); AsPh₃ (Triphenyl arsine); py (pyridine)

Scheme 2. Formation of ruthenium(II) Schiff base complexes.

511. ¹H NMR (ppm); 8.93(1H, s, HC=N), 7.26–7.70 (m, Ar-H). ¹³C NMR (ppm); 160 (C=N imine), 171 (C=N thiazole), 192 (C=O), 127–133 (Ar-C).

2.7. DNA-binding and cleavage assay

2.7.1. Electronic absorption spectroscopy

Electronic absorption titration of the ligand and its complexes were carried out in aqueous buffer solution (50 mM NaCl, 5 mM Tris-HCl, pH 7.1) at fixed complex concentration (10 μM) while gradually increasing the concentration of CT-DNA. The absorption data were analyzed to evaluate the intrinsic binding constant K_b, which can be determined from the following equation, [24]

$$[\text{DNA}]/(\epsilon_a - \epsilon_f) = [\text{DNA}]/(\epsilon_b - \epsilon_f) + 1/k_b(\epsilon_b - \epsilon_f)$$

where [DNA] is the concentration of DNA in base pairs, the apparent absorption coefficient ε_a, ε_f and ε_b correspond to A_{obsd}/[complex], the extinction coefficient of the free compound and the extinction coefficient of the compound when fully bound to DNA respectively. In plots of [DNA]/(ε_a-ε_f) vs [DNA], K_b is given by the ratio of slope to the intercept.

2.7.2. DNA cleavage

The DNA cleavage activity of the Schiff base metal complexes was monitored by agarose gel electrophoresis on CT DNA. The tests were performed under aerobic condition with H₂O₂ as an oxidant. Each reaction mixture contained 30 μM of CT DNA, 30 and 60 μM of each complex in DMSO and 60 μM of hydrogen peroxide in 50 mM Tris-HCl, (pH 7.1). The reaction was incubated at 37 °C for 2 h. After incubation, 1 μl of loading buffer (0.25% bromophenol blue, 0.25% xylene cynol and 60% glycerol) was added to the reaction mixture and loaded onto a 1% agarose gel containing 1.0 μg/ml of ethidium bromide. The electrophoresis was carried out for 2 h at 50 V in Tris-acetic acid EDTA buffer. The bands were visualized under UV light and photographed.

2.8. Cytotoxicity assay

The human cervical cancer cell line (HeLa) and human laryngeal epithelial carcinoma cell line (HEp2) was obtained from National Centre for Cell Science (NCCS), Pune, and grown in Eagles Minimum Essential Medium containing 10% fetal bovine serum (FBS). All cells were maintained at 37 °C, 5% CO₂, 95% air and 100% relative humidity. Maintenance cultures were passaged weekly, and the culture medium was changed twice a week.

The monolayer cells were detached with trypsin-ethylenediaminetetraacetic acid (EDTA) to make single cell suspensions and viable cells were counted using a hemocytometer and diluted with medium with 5% FBS to give final density of 1 × 10⁵ cells/ml. one hundred microlitres per well of cell suspension were seeded into 96-well plates at plating density of 10,000 cells/well and incubated to allow for cell attachment at 37 °C, 5% CO₂, 95% air and 100% relative humidity. After 24 h the cells were treated with serial concentrations of the extracts and fractions. They were initially dissolved in neat dimethylsulfoxide (DMSO) and further diluted in serum free medium to produce various concentrations. One hundred microlitres per well of each concentration was added to plates to obtain final concentrations of 1.0, 0.5, 0.25, 0.125, and 0.063 μg/ml. The final volume in each well was 200 μl and the plates were incubated at 37 °C, 5% CO₂, 95% air and 100% relative humidity for 48 h. The medium containing without samples were served as control. Triplicate was maintained for all concentrations.

MTT is a yellow water soluble tetrazolium salt. A mitochondrial enzyme in living cells, succinate-dehydrogenase, cleaves the tetrazolium ring, converting the MTT to an insoluble purple formazan.

Therefore, the amount of formazan produced is directly proportional to the number of viable cells.

After 48 h of incubation, 15 μ l of MTT (5 mg/ml) in phosphate buffered saline (PBS) was added to each well and incubated at 37 $^{\circ}$ C for 4 h. The medium with MTT was then flicked off and the formed formazan crystals were solubilized in 100 μ l of DMSO and then measured the absorbance at 570 nm using micro plate

reader. The % cell inhibition was determined using the following formula.

$$\% \text{Growth Inhibition} = 100 - \text{Abs}(\text{sample})/\text{Abs}(\text{control}) \times 100.$$

Nonlinear regression graph was plotted between % cell inhibition and Log_{10} concentration and IC_{50} was determined using GraphPad Prism software [25,26].

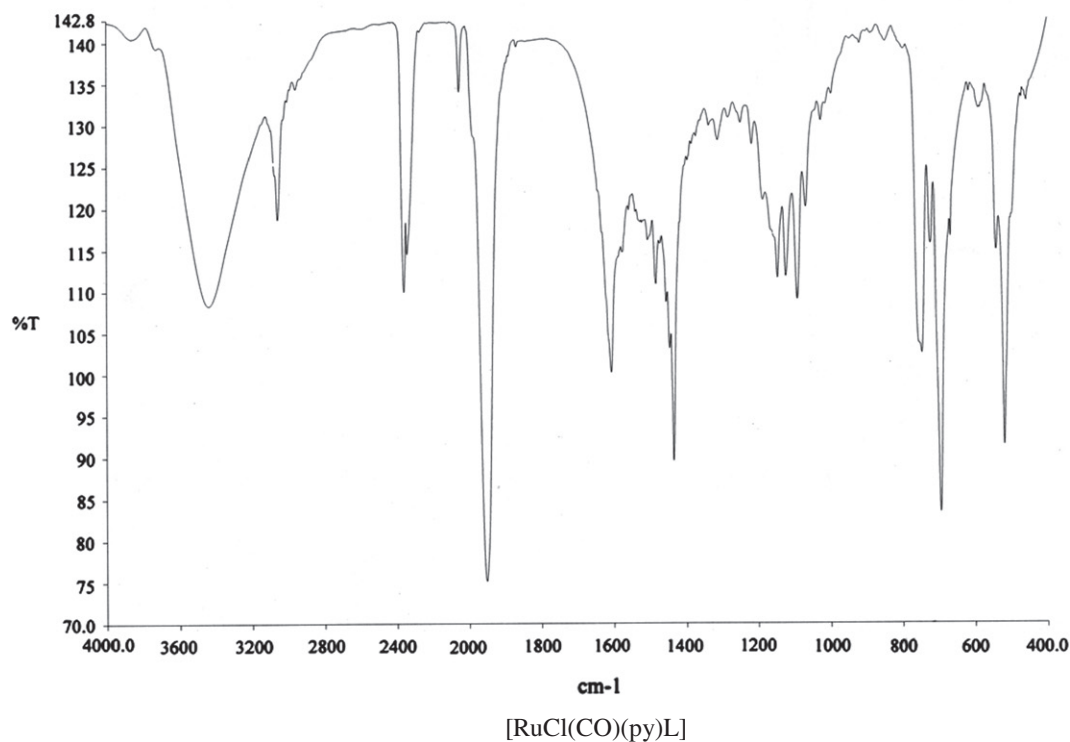
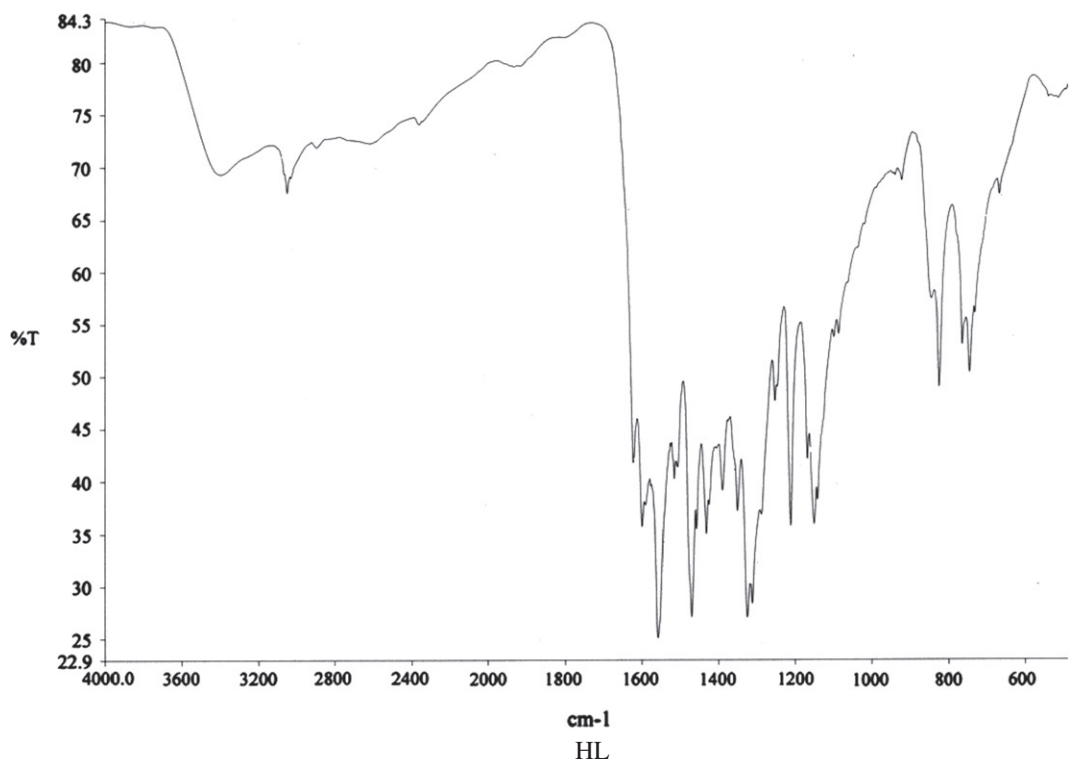


Fig. 2. IR Spectra of ligand HL and Complex [RuCl(CO)(py)L].

3. Results and discussion

3.1. Crystal structure of 3-(benzothiazol-2-yliminomethyl)-naphthalen-2-ol (HL)

The molecular structure of HL, along with the atom numbering scheme is given in Fig. 1.

The crystal data and structural refinement parameters are given in Table 1 and selected bond lengths and angles are given in Table 2. The compound crystallized into a monoclinic lattice with space group $P 2_1/n$. The azomethine bond, C12–N1 1.3943(19) Å is in conformity with a formal C=N double bond and the C1–O1 bond distance of 1.3348(18) Å, slightly shorter than the normal C–O single bond distance. The bond distance for C12–N2 1.2941(19) Å and C12–S1 1.7462(14) Å for thiazole group are closer to C–N and the C–S single bond, respectively. The single crystal X-ray diffraction study on his compound exits in imine-ol form without any ambiguity.

3.2. Spectroscopic data

3.2.1. Infrared spectra

The important IR spectral data of the ligand were compared with those of the ruthenium(II) complexes in order to confirm the binding mode of the Schiff base ligand to ruthenium ion in the complexes were shown Fig. 2. IR spectra of the Schiff base (HL) has the most characteristic bands appeared at 3396 cm^{-1} $\nu(\text{O–H})$, 1622 cm^{-1} $\nu(\text{C=N azomethine})$, 1599 cm^{-1} $\nu(\text{C=N thiazole ring})$, 1311 cm^{-1} $\nu(\text{ph-CO})$, and 744 cm^{-1} $\nu(\text{C–S–C})$. The band at 1622 cm^{-1} due to $\nu(\text{C=N})$ azomethine group of the Schiff base underwent a shift to lower frequency ($1618\text{--}1598\text{ cm}^{-1}$) after complexation, indicating the bonding of unsaturated nitrogen of the azomethine group to the metal ion [27]. The phenolic C–O stretching vibrations that appeared at 1311 cm^{-1} in the Schiff base [28] underwent a shift towards higher frequencies in the complexes. This shift confirms the participation of oxygen in the C–O–M bond. In the low frequency region $430\text{--}470\text{ cm}^{-1}$ is attributed to (M–O) and the region $560\text{--}580\text{ cm}^{-1}$ to (M–N) [29]. IR spectrum of the ligand of revealed a medium band at 1599 cm^{-1} (C=N) thiazole ring, which is shifted to lower frequency at about ($1578\text{--}1573\text{ cm}^{-1}$) after complexation, which also indicates that it has been affected upon coordination to ruthenium metal ions. The unchanged band after complexation at 748 cm^{-1} in the free ligand suggests non-involvement of the coordination which was assigned to $\nu(\text{C–S–C})$. In all the complexes, the strong band in the region $1963\text{--}1925\text{ cm}^{-1}$ is due to terminally coordinated carbonyl group. For the complex $[\text{RuCl}(\text{CO})(\text{py})\text{L}]$, the IR spectrum showed a medium intensity band at 1119 cm^{-1} which is characteristics of coordinated nitrogen base. Characteristic bands for triphenyl phosphine/arsine are also present in the expected region [30].

3.2.2. Electronic spectra

The electronic spectra of the Schiff base HL and its complexes were taken in DMSO and shown in Fig. 3. Two very strong bands at 365 and 276 nm were observed in the spectra of the ligand, which is attributed to $n\text{--}\pi^*$ and $\pi\text{--}\pi^*$ transitions in the aromatic ring and C=N chromophore [31]. The electronic spectra of all complexes showed five bands in the region 252–531 nm. All the ruthenium(II) complexes in an octahedral environment is $^1A_{1g}$ arising from the t_{2g}^6 configuration and the excited states corresponding to the $t_{2g}^5 e_g^1$ configuration are $^3T_{1g}$, $^3T_{2g}$, $^1T_{1g}$ and $^1T_{2g}$. Hence, four bands corresponding to the transition $^1A_{1g} \rightarrow ^3T_{1g}$, $^1A_{1g} \rightarrow ^3T_{2g}$, $^1A_{1g} \rightarrow ^1T_{1g}$ and $^1A_{1g} \rightarrow ^1T_{2g}$ are possible in order of increasing energy. The low energy bands in the visible region are assigned to the charge transfer (CT) transitions. The charge transfer bands ob-

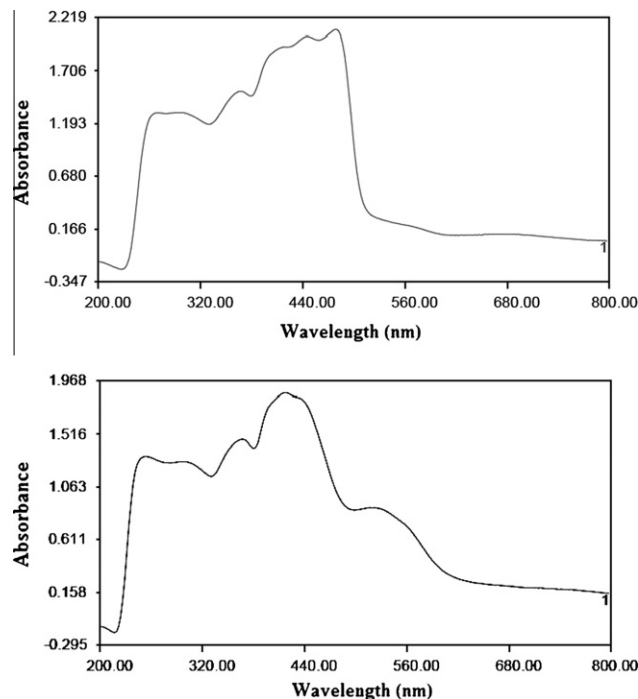


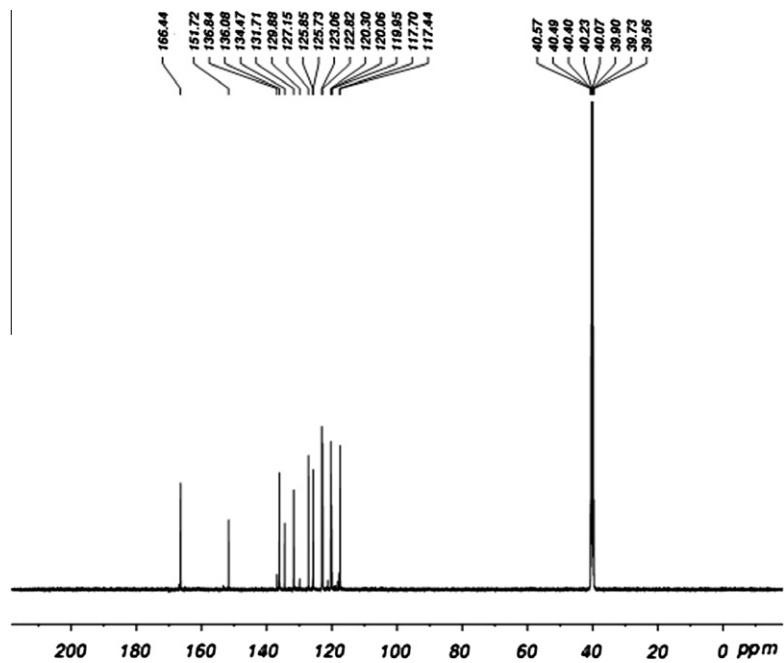
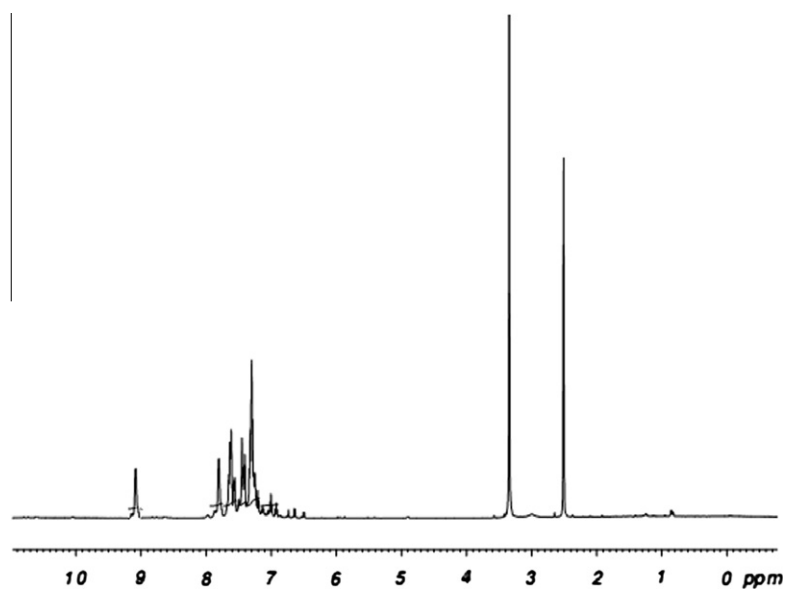
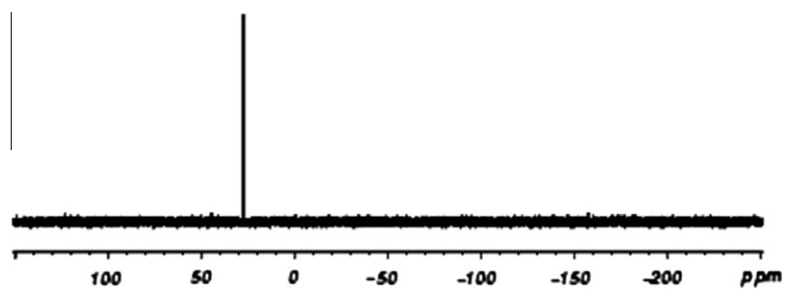
Fig. 3. UV-visible spectra of ligand HL and Complex $[\text{RuCl}(\text{CO})(\text{PPh}_3)\text{L}]$.

served in all the complexes due to $M \rightarrow L$ transitions are possible in the visible region in the range of 416–531 nm [32–34]. The other bands in the region 252–365 nm region were assignable to ligand centered (LC) transitions and have been designated as $\pi\text{--}\pi^*$ and $n\text{--}\pi^*$ transition. The pattern of the electronic spectra of all the complexes indicated the presence of an octahedral environment around the ruthenium(II) ion, similar to that of other ruthenium(II) octahedral complexes [35].

3.2.3. NMR spectra

The ^1H NMR spectra of ligand and complexes were recorded in DMSO- d_6 solution for confirming the binding mode of the Schiff base to ruthenium ion shown in Figs. 4–6. The aromatic protons for the ligand appeared as a multiplet at 7.24–8.27 ppm. On complexation, the protons on the phenyl ring remain more or less unchanged in the complexes, even if there are slight variation in their resonances due to the delocalization of electron density in the system [36] and these signals in the complexes cannot be distinguished from the aromatic signals of $\text{PPh}_3/\text{AsPh}_3$ due to their extensive overlap appeared at 7.26–8.12 ppm [37]. The proton of the hydroxyl group appears as broad singlet at 10.12 (Ph-OH) ppm for free Schiff base ligand. In the spectra of the complexes, the resonance arising from the hydroxyl (Ph-OH) proton is not observed, indicating the coordination of the hydroxyl oxygen to the metal ion [8]. The signal due to the azomethine proton (–HC=N) is found to be considerably deshielded at 8.93–9.12 ppm relatively to that of the free Schiff base ligand 8.72 ppm as a consequence of electron donation to the metal center.

The ^{13}C NMR data were recorded in DMSO- d_6 solution and the assignment of ligand and the complexes are given. ^{13}C NMR spectra of all Schiff base ligand displayed a single resonance at 152 ppm [38] showed that the azomethine carbon atoms were equivalent, which also confirm the structure of the ligand. The signal at 166 ppm corresponds to thiazolic C=N carbon [39]. The downfield shift of these two signals at 162–159 and 169–171 ppm clearly indicates that both the C=N carbons were affected by coordination [40]. The aromatic carbons of free ligand and the corresponding

Fig. 4. ^{13}C NMR spectrum of HL.Fig. 5. ^1H NMR spectrum of $[\text{RuCl}(\text{CO})(\text{PPh}_3)_3\text{L}]$.Fig. 6. ^{31}P NMR spectrum of $[\text{RuCl}(\text{CO})(\text{PPh}_3)_3\text{L}]$.

complexes show signals in the region 114–138 ppm. For all the complexes, the terminal carbonyl group appeared in the range 191–194 ppm [41].

In order to confirm the presence of triphenylphosphine group and to determine the geometry of the complexes ^{31}P NMR spectra were recorded. ^{31}P NMR spectra of the complex $[\text{Ru}(\text{CO})\text{Cl}(\text{PPh}_3)\text{L}]$ and $[\text{Ru}(\text{CO})\text{Cl}(\text{py})\text{L}]$ were recorded in $\text{DMSO}-d_6$ solution. The observation of a sharp singlet at 28.2 ppm for the complex $[\text{Ru}(\text{CO})\text{Cl}(\text{PPh}_3)\text{L}]$ confirms the presence of only one triphenylphosphine group. No signals were observed for complex $[\text{Ru}(\text{CO})\text{Cl}(\text{py})\text{HL}]$ confirms the absence of phosphine group.

3.3. DNA binding and cleavage

3.3.1. Electronic absorption spectroscopy

Electronic absorption spectroscopy is one of the most useful techniques for DNA-binding studies of metal complexes. The interaction of ruthenium complexes with CT-DNA were investigated by UV absorption titrations. The binding of the ruthenium complexes to DNA helices was characterized by following the changes in the absorbance and shift in wavelength on each addition of DNA solution to the complex. The ruthenium(II) complexes in DMSO -buffer mixture exhibit an intense transition in the region around 348–252 nm, which is attributed to a $\pi-\pi^*$ intraligand transition that unique to this Schiff base. On the titration of CT-DNA with the Schiff base ligand and complexes, a considerable increase or decrease in the absorption along with small blue shift was observed. With increasing concentration of DNA, the absorption bands of the ligand and complexes were affected to a considerable extent. For ligand and complexes, the absorption spectra show clearly that the addition of DNA to the complexes yields hyperchromism and a blue shift to the ratio of $[\text{DNA}]/[\text{Ru}]$. Obviously, these spectral characteristics suggest that all the complexes interact with DNA most likely through a mode that involves a stacking interaction between the aromatic chromophore and the base pairs of DNA. Addition of increasing amounts of DNA resulted in hypsochromism of the peak maxima in the UV-visible spectra of the ligand and complexes Figs. 7–10. Complex interaction occurs with exterior phosphates of DNA via., electrostatic attraction [42]. In the plot of $[\text{DNA}]/(\epsilon_a - \epsilon_f)$ vs $[\text{DNA}]$, the binding constant K_b is given by the ratio of the slope to the y intercept. The intrinsic binding constant (K_b) of ligand, (1) and (3) are of $1.4 \times 10^4 \text{ M}^{-1}$, $4.9 \times 10^4 \text{ M}^{-1}$, $7.2 \times 10^4 \text{ M}^{-1}$. The DNA-binding constant of the title complexes are comparable to those of some polypyridyl Ru(II) complexes $1.0\text{--}4.8 \times 10^4 \text{ M}^{-1}$ [43,44].

As the concentration of the DNA was increased, the absorption bands of $[\text{RuCl}(\text{CO})(\text{AsPh}_3)(\text{HL})]$ (2) showed hyperchromism initially and on further increment, hypochromism of with a blue shift (5 nm) was observed. An isosbestic point was observed at 265 nm.

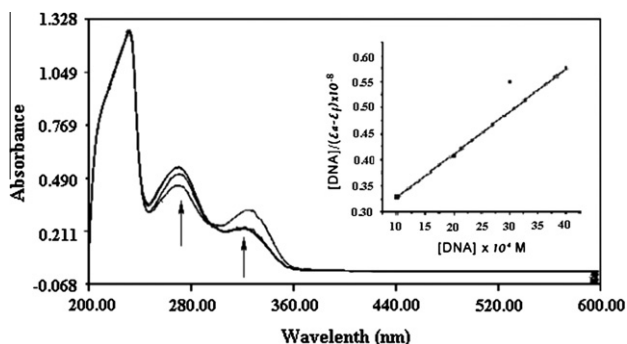


Fig. 7. Electronic absorption spectra of the Schiff base ligand (HL) in the absence and presence of increasing amount of CT-DNA.

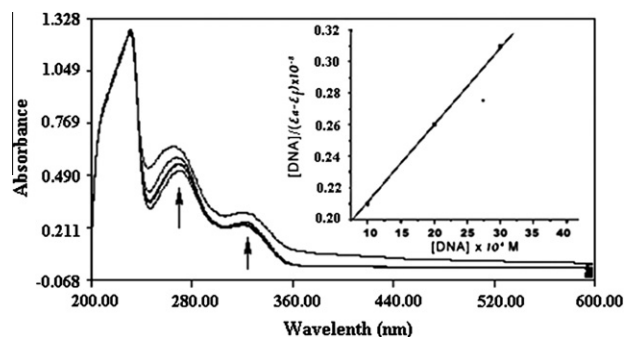


Fig. 8. Electronic absorption spectra of the complex 1 in the absence and presence of increasing amount of CT-DNA.

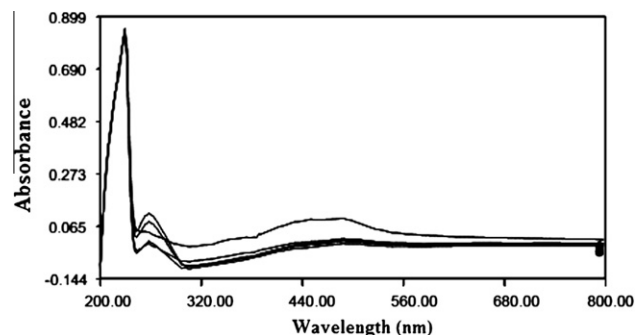


Fig. 9. Electronic absorption spectra of the complex 2 in the absence and presence of increasing amount of CT-DNA.

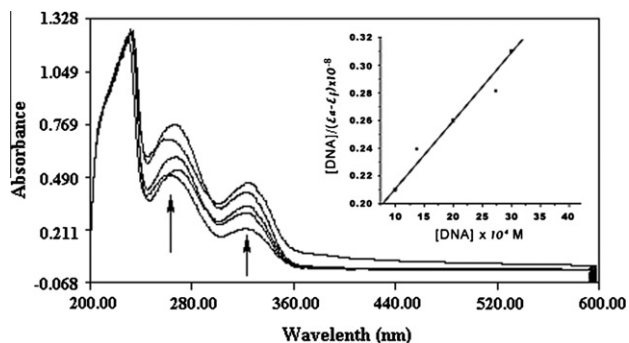


Fig. 10. Electronic absorption spectra of the complex 3 in the absence and presence of increasing amount of CT-DNA.

This behavior reveals an electrostatic association of the complex with the helix surface [45]. Hyperchromicity and hypochromicity is the spectral feature of DNA concerning its double helix structure [46]. Hyperchromic effect reflects the corresponding changes of DNA in its conformation and structure after the complexes are bound to DNA. Hypochromism results from contraction of DNA in the helix axis while hyperchromism results from the damage of DNA helix structure. The binding constant of the complex 2 could not be evaluated due to the random changes in the absorption on the addition of DNA.

3.3.2. DNA cleavage activity

The cleavage efficiency of the complexes compared with that of the control is due to their efficient DNA-binding ability. The metal complexes were able to convert super coiled DNA into open circular DNA. The general oxidative mechanisms proposed account for

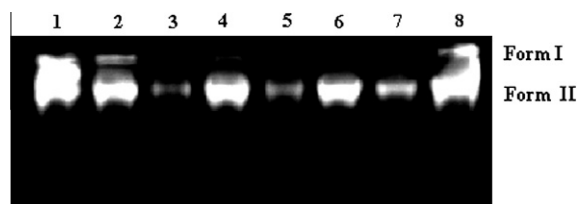


Fig. 11. Gel electrophoresis showing the chemical nuclease activity of the CT-DNA incubated at 37 °C for 2 h with different concentration of complex 1, 2 and 3 in the presence of H₂O₂ as an oxidant ; lane 1, DNA control; lane 2, DNA + H₂O₂ (60 μM) + complex 1 (30 μM); lane 3, DNA + H₂O₂ (60 μM) + complex 1 (60 μM); lane 4, DNA + H₂O₂ (60 μM) + complex 2 (30 μM); lane 5, DNA + H₂O₂ (60 μM) + complex 2 (60 μM); lane 6, DNA + H₂O₂ (60 μM) + complex 3 (30 μM); lane 7, DNA + H₂O₂ (60 μM) + complex 3 (60 μM); lane 8, DNA + H₂O₂ (60 μM).

DNA cleavage by hydroxyl radicals *via.*, abstraction of a hydrogen atom from sugar units and predict the release of specific residues arising from transformed sugars, depending on the position from which the hydrogen atom is removed [47].

In the present study, the CT-DNA gel electrophoresis experiment was conducted at 35 °C using our synthesized ruthenium(II) complexes in the presence of H₂O₂ as an oxidant. It was found that, at very low concentrations, few complexes exhibit nuclease activity in the presence of H₂O₂. Control experiment using DNA alone does not show any significant cleavage of CT-DNA even on longer exposure time. Hence, we conclude that the ruthenium(II) complex cleaves DNA at different concentrations as compared with control DNA Fig. 10. The amount of Form I diminished gradually, partly converted to Form II, where as the intensity of the Form II band increased as the concentration of the ruthenium(II) complexes as increased, showing the potential chemical nuclease activity of the complexes. When the concentration increased to 60 μM for all the complexes, DNA was completely converted from Form I to Form II. The result showed that complex 1 has more cleavage activity than other complexes (see Fig. 11).

3.4. Cytotoxic activity evaluation

To test the cytotoxicity of Schiff base ligand and ruthenium(II) complexes, human cervical cancer cell line (HeLa) and the human laryngeal epithelial carcinoma cell line (HEp2) were cultured in the presence of varying concentrations of ligand and corresponding ruthenium(II) complexes for 48 h. The inhibitory concentration 50 (IC₅₀), defined as the concentration required to reduce the size of the cell population by 50%. The IC₅₀ values obtained of ligand and its complexes against selected two tumor cell lines are given in Table 3. The IC₅₀ values of the ligand (IC₅₀ = 175 μM) exhibit enhanced activity against HeLa cell line and low activity (IC₅₀ = 389 μM) against HEp2. The IC₅₀ values are 149, 244 μM for complex 1, 123, 212 μM for complex 2 and 87, 149 μM for complex 3 against HeLa and HEp2 cell lines. All the ruthenium(II) complexes show significant activity against the two tumor cell lines. Thus, the IC₅₀ value for the ligand decreases with the coordination of it to ruthenium metal which shows the more toxicity of the complexes

Table 3
The IC₅₀ values for Schiff base ligand and ruthenium(II) complexes against selected cell lines.

Compound	HeLa	HEp2
HL	175 μM	>300 μM
Complex 1	149 μM	244 μM
Complex 2	123 μM	212 μM
Complex 3	87 μM	149 μM

than the ligand. However, these values are lower than the standard anticancer drug cisplatin [48].

4. Conclusion

Three ruthenium(II) complexes containing 3-(benzothiazol-2-yliminomethyl)-naphthalen-2-ol ligand, were synthesized and characterized by various spectroscopic techniques. Schiff base ligand has also been characterized crystallographically. All the newly synthesized complexes and ligand were evaluated for DNA-binding, DNA cleavage and cytotoxicity studies. DNA-binding behaviors were examined by absorption spectroscopy. The results indicate that intrinsic binding constant of complex 1, 3 and ligand varies in the range of 1.4–7.2 × 10⁴ M⁻¹. Complex 2 on the other hand shows dual mode of binding to DNA. The complexes and ligand behave as a DNA groove binder. DNA cleavage studies revealed that all the three complexes have the ability to cleave nucleic acids and the extent of the cleavage was found to be dose dependent. Cytotoxicity evaluation *in vitro* shows that complex 3 displayed better antitumor activity against selected cell lines. The ligand and complexes 1 and 2 shows moderate antitumor activity.

Supplementary material

Crystallographic data for the structural analysis have been deposited with the Cambridge Crystallographic Data Centre, CCDC 814145. Copy of this information may be obtained free of charge from the Director, CCDC, 12 Union Road, Cambridge, CB21 2EZ, UK (fax: +44 1223 336033; e-mail: deposit@ccdc.cam.ac.uk or www.ccdc.cam.ac.uk/deposit).

Acknowledgements

We sincerely thank University Grants Commission (UGC), New Delhi for financial support [Scheme. No. 38-222/2009 (SR)]. One of the author RJB wishes to acknowledge the NSF-MRI program (grant No. CHE-0619278) for providing funds to purchase the diffractometer.

References

- [1] Y.-M. Song, Q. Wu, P.-J. Yang, N.-N. Luan, L.-F. Wang, Y.-M. Liu, *J. Inorg. Biochem.* 100 (2006) 1685.
- [2] M. Kozurkova, D. Sabolova, L. Janovec, J. Mikes, J. Koval, J. Ungvarsky, M. Stefanisinova, P. Fedorocko, P. Kristian, J. Imrich, *Bioorg. Med. Chem.* 16 (2008) 3976.
- [3] C.-P. Tan, J. Liu, L.-M. Chen, S. Shi, L.-N. Ji, *J. Inorg. Biochem.* 102 (2008) 1644.
- [4] G. Zuber, J.C. Quada Jr, S.M.J. Hecht, *Am. Chem. Soc.* 120 (1998) 9368.
- [5] S.M.J. Hecht, *Nat. Prod.* 63 (2000) 158.
- [6] C. Metcalfe, J.A. Thomas, *Chem. Soc. Rev.* 32 (2003) 215.
- [7] A. Silvestri, G. Barone, G. Ruisi, M.T. Lo Giudice, S.J. Tumminello, *Inorg. Biochem.* 98 (2004) 589.
- [8] M. Navarro, E.J. Cisneros-Fajardo, A. Sierralta, M. Fernández-Mestre, P. Silva, D. Arrieché, E. Marchán, *J. Biol. Inorg. Chem.* 8 (2003) 401.
- [9] H. Xu, K.-C. Zheng, H. Deng, L.-J. Lin, Q.-L. Zhang, L.-N. Ji, *Dalton. Trans.* 3 (2003) 2260.
- [10] H. Xu, K.-C. Zheng, H. Deng, L.-J. Lin, Q.-L. Zhang, L.-N. Ji, *New J. Chem.* 27 (2003) 1255.
- [11] M. Asadi, E. Safaei, B. Ranjbar, L. Hasani, *New J. Chem.* 28 (2004) 1227.
- [12] S.R. Collinson, D.E. Fenton, *Coord. Chem. Rev.* 148 (1996) 19.
- [13] A.K. Sharma, S. Chandra, *Spectrochim. Acta A* 78 (2011) 337.
- [14] H.F. Abd El-halim, M.M. Omar, G.G. Mohamed, *Spectrochim. Acta A* 78 (2011) 36.
- [15] T.B.S.A. Ravooof, K.A. Crouse, M.I.M. Tahir, F.N.F. How, R. Rosli, D.J. Watkins, *Trans. Met. Chem.* 35 (2010) 871.
- [16] N.P. Priya, S. Arunachalam, A. Manimaran, D. Muthupriya, C. Jayabalakrishnan, *Spectrochim. Acta A* 72 (2009) 6706.
- [17] V. Beneteau, T. Besson, J. Guillard, S. Leonce, B. Pfeiffer, *Eur. J. Med. Chem.* 34 (1999) 1053.
- [18] G. Sathiyaraj, T. Weyhermuller, B.U. Nair, *Eur. J. Med. Chem.* 45 (2010) 284.
- [19] I. Sakyan, E. Logoglu, S. Arslan, N. Sari, N. Sakiyan, *Bio Metals.* 17 (2004) 115.
- [20] G.M. Sheldrick, SHELXS -97 SHELXL -97 Fortran Programs for Crystal Structure Solution and Refinement, University of Gottingen, Germany, 1997.

- [21] N. Ahmed, J.J. Levison, S.D. Robinson, M.F. Uttley, *Inorg. Synth.* 15 (1974) 48.
- [22] R.A. Sanchez-Delgado, W.Y. Lee, S.R. Choi, Y.M.J. Cho, Y. Jun, *Trans. Met. Chem.* 16 (1991) 41.
- [23] S. Gopinathan, I.R. Unny, S.S. Deshpande, C. Gopinathan, *Ind. J. Chem. A* 25 (1986) 1015.
- [24] A. Wolf, G.H. Shimer, T. Meehan, *Biochemistry* 26 (1987) 6392.
- [25] T. Mosmann, *J. Immunol. Methods* 65 (1983) 55.
- [26] A. Monks, *J. Natl Cancer Inst.* 83 (1991) 757.
- [27] R. Ramesh, M. Sivagamasundari, *Synth. React. Inorg. Met-Org. Chem.* 33 (2003) 899.
- [28] R.C. Maurya, P. Patel, S. Rajput, *Synth. React. Inorg. Met-org. Chem.* 23 (2003) 817.
- [29] K. Nakamoto, *Infrared and Raman spectra of Inorganic and Co-ordination compounds*, Wiley Interscience, New York, 1971.
- [30] A.K. Das, S.M. Peng, S.J. Bhattacharya, *Chem. Soc. Jpn.* 49 (1976) 287.
- [31] R.K. Sharma, R.V. Singh, J.P.J. Tandon, *Inorg. Nucl. Chem.* 42 (1980) 1382.
- [32] K. Natarajan, R.K. Poddar, C.J. Agarwala, *Inorg. Nucl. Chem.* 39 (1977) 431.
- [33] A.B.P. Lever, *Inorganic Electronic Spectroscopy*, 2nd ed., Elsevier, New York, 1984.
- [34] K. Chichak, U. Jacquenard, N.R. Branda, *Eur. J. Inorg. Chem.* (2002) 357.
- [35] P. Sengupta, R. Dinda, S. Ghosh, *Trans. Met. Chem.* 27 (2002) 665.
- [36] M. Maji, S. Ghosh, S.K. Chattopaghyay, T.C.W. Mak, *Inorg. Chem.* 36 (1997) 2938.
- [37] R.V. Singh, S.C. Joshi, A. Gajraj, P. Nagpal, *Appl. Organomet. Chem.* 16 (2002) 713.
- [38] J.T. Desai, C.K. Desai, K.R.I. Desai, *Iran. Chem. Soc.* 5 (2008) 67.
- [39] S. Perz, C. Lopez, A. Caubet, X. Solans, M.F. Bardia, M. Gich, E. Molins, *J. Organomet. Chem.* 692 (2007) 2402.
- [40] K. Shankera, R. Rohinia, V. Ravindera, P.M. Reddy, Y.-P. Ho, *Spectrochim. Acta A* 73 (2009) 205.
- [41] M.H. Desbosis, D. Astruc, *Organometallics* 8 (1989) 1841.
- [42] M. Chauhan, F.J. Arjmand, *Organomet. Chem.* 692 (2007) 5156.
- [43] X.W. Liu, J. Li, H. Deng, K.C. Zheng, Z.W. Mao, L.N. Ji, *Inorg. Chim. Acta.* 358 (2005) 3311.
- [44] X.H. Zao, B.H. Ye, H. Li, Q.L. Zhang, H. Chao, J.G. Liu, L.N. Ji, X.Y. Li, *J. Biol. Inorg. Chem.* 6 (2001) 143.
- [45] D. Herebian, W.S.J. Sheldrick, *Chem. Soc. Dalton Trans.* (2002) 966.
- [46] Q.S. Li, P. Yang, H.F. Wang, M.L. Guo, *J. Inorg. Biochem.* 64 (1996) 181.
- [47] G. Pratiel, M. Pitie, J. Bernadou, B. Meunier, *Angew. Chem. Int. Ed. Eng.* 30 (1991) 702.
- [48] Y.-J. Liu, C.-H. Zeng, Z.-H. Liang, J.-H. Yao, H.-L. Huang, Z.-Z. Li, F.-H. Wu, *Eur. J. Med. Chem.* 45 (2010) 3087.